

Systems biology

# Network-based prediction of drug–target interactions using an arbitrary-order proximity embedded deep forest

Xiangxiang Zeng <sup>1,†</sup>, Siyi Zhu<sup>2,†</sup>, Yuan Hou<sup>3</sup>, Pengyue Zhang<sup>4</sup>, Lang Li<sup>4</sup>, Jing Li<sup>5</sup>, L. Frank Huang<sup>6,7</sup>, Stephen J. Lewis<sup>8</sup>, Ruth Nussinov<sup>9,10</sup> and Feixiong Cheng <sup>3,11,12,\*</sup>

<sup>1</sup>Department of Computer Science, College of Information Science and Engineering, Hunan University, Changsha, Hunan 410082, China, <sup>2</sup>Department of Computer Science, Xiamen University, Xiamen 361005, China, <sup>3</sup>Genomic Medicine Institute, Lerner Research Institute, Cleveland Clinic, Cleveland, OH 44195, USA, <sup>4</sup>Department of Biomedical Informatics, Ohio State University, Columbus, OH 43210, USA, <sup>5</sup>Department of Computer and Data Sciences, Case Western Reserve University, Cleveland, OH 44106, USA, <sup>6</sup>Division of Experimental Hematology and Cancer Biology, Brain Tumor Center, Cincinnati Children's Hospital Medical Center and <sup>7</sup>Department of Pediatrics, University of Cincinnati College of Medicine, Cincinnati, OH 45229, USA, <sup>8</sup>Department of Pediatrics, Case Western Reserve University, Cleveland, OH 44106, USA, <sup>9</sup>Computational Structural Biology Section, Basic Science Program, Frederick National Laboratory for Cancer Research, National Cancer Institute at Frederick, Frederick, MD 21702, USA, <sup>10</sup>Department of Human Molecular Genetics and Biochemistry, Sackler School of Medicine, Tel Aviv University, Tel Aviv 69978, Israel, <sup>11</sup>Department of Molecular Medicine, Cleveland Clinic Lerner College of Medicine, Case Western Reserve University, Cleveland, OH 44195, USA and <sup>12</sup>Case Comprehensive Cancer Center, Case Western Reserve University School of Medicine, Cleveland, OH 44106, USA

\*To whom correspondence should be addressed.

<sup>†</sup>The authors wish it to be known that, in their opinion, the first two authors should be regarded as Joint First Authors.

Associate Editor: Pier Luigi Martelli

Received on September 18, 2019; revised on December 24, 2019; editorial decision on January 1, 2020; accepted on January 17, 2020

## Abstract

**Motivation:** Systematic identification of molecular targets among known drugs plays an essential role in drug repurposing and understanding of their unexpected side effects. Computational approaches for prediction of drug–target interactions (DTIs) are highly desired in comparison to traditional experimental assays. Furthermore, recent advances of multiomics technologies and systems biology approaches have generated large-scale heterogeneous, biological networks, which offer unexpected opportunities for network-based identification of new molecular targets among known drugs.

**Results:** In this study, we present a network-based computational framework, termed AOPEDF, an arbitrary-order proximity embedded deep forest approach, for prediction of DTIs. AOPEDF learns a low-dimensional vector representation of features that preserve arbitrary-order proximity from a highly integrated, heterogeneous biological network connecting drugs, targets (proteins) and diseases. In total, we construct a heterogeneous network by uniquely integrating 15 networks covering chemical, genomic, phenotypic and network profiles among drugs, proteins/targets and diseases. Then, we build a cascade deep forest classifier to infer new DTIs. Via systematic performance evaluation, AOPEDF achieves high accuracy in identifying molecular targets among known drugs on two external validation sets collected from DrugCentral [area under the receiver operating characteristic curve (AUROC) = 0.868] and ChEMBL (AUROC = 0.768) databases, outperforming several state-of-the-art methods. In a case study, we show-case that multiple molecular targets predicted by AOPEDF are associated with mechanism-of-action of substance abuse disorder for several marketed drugs (such as aripiprazole, risperidone and haloperidol).

**Availability and implementation:** Source code and data can be downloaded from <https://github.com/ChengF-Lab/AOPEDF>.

**Contact:** chengf@ccf.org

**Supplementary information:** [Supplementary data](#) are available at *Bioinformatics* online.

## 1 Introduction

Identification of drug–target interactions (i.e. interactions between drugs and targets/proteins; DTIs) plays an important role in drug discovery and development. Since experimental determination of DTIs is costly and time-consuming (Haggarty *et al.*, 2003; Kuruvilla *et al.*, 2002), *in silico* or computational approaches have offered possibilities to identify potential DTIs for accelerating drug development, such as drug repurposing. Several *in silico* approaches, such as structure-based (Donald, 2011; Morris *et al.*, 2009), ligand-based (Keiser *et al.*, 2007) and machine learning-based methods (Bleakley and Yamanishi, 2009; Wan *et al.*, 2019), have revealed potential in predicting DTIs. However, structure-based methods are limited when 3D structures of proteins are unavailable (Cheng *et al.*, 2007; Rarey *et al.*, 1996) which, unfortunately, is the case for the majority of targets. Ligand-based methods exploit the chemical structures of ligands to make predictions, and their performance is poor when the chemical space of the ligands is out of application domains. A variety of machine learning-based approaches have been developed to predict DTIs (Bleakley and Yamanishi, 2009; He *et al.*, 2010; Mei *et al.*, 2013; Perlman *et al.*, 2011; Xia *et al.*, 2010). These methods fully exploit latent correlations among the related features of drugs and targets and offer moderate accuracy for prediction of DTIs. Altogether, most existing methods for DTI prediction are limited to homogeneous networks or bipartite drug–target networks (Cheng *et al.*, 2012a) and cannot be directly extended to heterogeneous, biological networks (Cheng *et al.*, 2012b).

In comparison to homogeneous networks, heterogeneous networks naturally assemble more objects and complementary information from drugs, targets/proteins and their associated diseases. Several computational approaches have recently been reported to integrate heterogeneous data sources. For example, MSCMF (Zheng *et al.*, 2013) integrates multiple data sources via a weighted averaging scheme and uses the resulting drug and protein similarity matrices to regularize the matrix factorization operation of a given DTI network. However, such data integration may cause substantial losses in network-specific information. HNM (Wang *et al.*, 2014) fuses heterogeneous data by a network diffusion process; however, directly using diffusion states as features or prediction scores may easily suffer from the bias introduced by the noise and high-dimensionality of biological network data. Inspired by the recent surge of deep learning techniques for feature extracting, models with higher predictive capacity have been explored. DeepWalk is a deep learning method by utilizing the similarities from a tripartite, heterogeneous network built from biomedical linked datasets (Zong *et al.*, 2017). NeoDTI integrated neighborhood information of the heterogeneous network and automatically learns topology-preserving representations of drugs and targets (Wan *et al.*, 2019). However, these methods are mainly based on a shallow neural network model with only three layers. Besides, these methods are prone to preserving only the first- or second-order proximity. deepDTnet (Zeng *et al.*, 2020) adopted deep autoencoder to automatically learn high-quality features from heterogeneous networks, and then applied positive-unlabeled (PU)-matrix completion to predict new DTIs. Yet, recent studies have suggested that high-order proximities among diverse types of nodes play crucial roles in capturing the underlying topological structure of the network (Cao *et al.*, 2015; Cui *et al.*, 2019; Perozzi *et al.*, 2014); further, embedding with certain order proximity does not necessarily perform best on all networks. We asserted that incorporating diverse, complementary proximities from different biological networks may improve accuracy further (Zhang *et al.*, 2018).

In this study, we propose arbitrary-order proximity embedded deep forest (AOPEDF), a new computational approach for molecular target identification from known drugs and for target-centered drug repurposing. Specifically, AOPEDF preserves the different order proximity information from 15 networks in a constructed

drug–target–disease heterogeneous network. It then utilizes low-dimensional but informative vector representations of features for both drugs and targets/proteins through a cascade deep forest classifier in prediction of DTIs. Theoretically, AOPEDF has the following advantages: (i) AOPEDF integrates diverse information from 15 heterogeneous networks and preserves complementary order proximity information for different networks. Thus, the low-dimensional feature vectors learned by AOPEDF capture rich context information as well as the topological structure of individual networks. (ii) AOPEDF adopts deep forest as a classifier, which achieves high performance in classification but has much fewer hyper-parameters than deep neural networks (DNN) (LeCun *et al.*, 2015). AOPEDF is highly robust to hyper-parameter settings. Importantly, the number of cascade levels can be adaptively determined such that the model complexity can be automatically set. (iii) Tree-based methods implemented in AOPEDF make prediction by inferring decision rules from data, which is more effective in generating interpretable predictions from rich features compared to traditional neural network methods. Via comprehensive evaluation on cross-validation and two external validation sets, we show that AOPEDF achieves higher performance in comparison to several state-of-the-art methods. In summary, AOPEDF offers a powerful tool to predict new DTIs from heterogeneous networks for accelerating target-centered drug repurposing and therapeutic development for understudied diseases.

## 2 Materials and methods

### 2.1 Data resource

We collect DTI information from the DrugBank database (v4.3) (Wishart *et al.*, 2018), the therapeutic target database (Yang *et al.*, 2016) and the PharmGKB database (Hernandez-Boussard *et al.*, 2007). Specifically, bioactivity data for drug–target pairs are collected from ChEMBL (v20) (Gaulton *et al.*, 2012), BindingDB (Liu *et al.*, 2007) and IUPHAR/BPS Guide to PHARMACOLOGY (Pawson *et al.*, 2014). The chemical structure of each drug with SMILES format is extracted from DrugBank (Law *et al.*, 2014). Here, only DTIs meeting the following three criteria are used: (i) the human target is represented by a unique UniProt accession number; (ii) the target is marked as ‘reviewed’ in the UniProt database (Apweiler *et al.*, 2004); and (iii) binding affinities, including  $K_i$ ,  $K_d$ , IC50 or EC50 each  $\leq 10 \mu\text{M}$ . We used a low binding affinity cutoff of  $10 \mu\text{M}$  as weak-binding drugs play crucial roles in therapeutic development as well (Ohlson, 2008; Wang *et al.*, 2017). In total, a DTI network connecting 732 FDA-approved drugs and 1519 unique human targets (proteins) were used (Supplementary Tables S1 and S2). We randomly selected the matching number of the unknown drug–target pairs (by excluding all known DTIs) as negative samples. The details for building the experimentally validated drug–target network are provided in a recent publication (Cheng *et al.*, 2018). In addition, we construct nine networks for drugs: (i) clinically reported drug–drug interactions, (ii) drug–disease associations, (iii) drug–side effect associations, (iv) chemical similarities, (v) therapeutic similarities derived from the Anatomical Therapeutic Chemical Classification System, (vi) target sequence-derived drug–drug similarities, (vii) Gene Ontology (GO) biological process, (viii) GO cellular component and (ix) GO molecular function, and six networks for proteins: (i) protein–protein interactions, (ii) protein–disease associations, (iii) protein sequence similarities, (iv) GO biological process, (v) GO cellular component and (vi) GO molecular function. The detailed description for building 15 networks is provided in the Supplementary Methods and our recent study (Cheng *et al.*, 2019a,b). For external validation sets, we assembled the newest experimentally validated DTIs from the DrugCentral database (Ursu *et al.*, 2019) and ChEMBL database (Mendez *et al.*, 2019) by excluding overlapping drug–target pairs from the training set. There

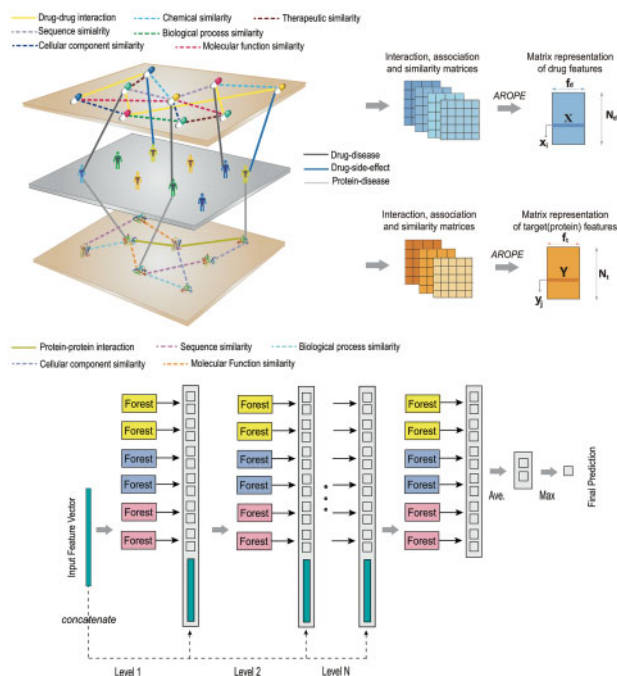


Fig. 1. A flowchart of the proposed approach. First, we integrate 15 networks to construct a complicated heterogeneous network which contains diverse chemoinformatics and bioinformatics profiles and a multiview perspective for predicting DTIs. Then, AOPEDF integrates diverse information from the heterogeneous network, and preserves the different order proximity information for different networks through AROPE. Finally, the deep forest classifier is utilized to infer potential DTIs among known drugs

are partly overlap between two validated sets from DrugCentral and ChEMBL databases, respectively (Supplementary Table S3). There are no any overlap DTIs between the training set and two external validation set.

## 2.2 Pipeline of AOPEDF

As shown in Figure 1, AOPEDF consists of three steps: (i) data preparation and benchmarking, (ii) arbitrary-order proximity preserved network embedding (AROPE) and (iii) deep forest-based prediction of DTIs. First, we integrate 15 biological networks to construct a complex heterogeneous network which contains diverse information and a multiview perspective in predicting novel DTIs. Then, we preserve arbitrary-order proximity of each network to obtain informative, but low-dimensional vector representations of drugs and targets. Finally, potential DTIs will be predicted using the deep forest classifier.

## 2.3 Arbitrary-order proximity preserved network embedding

We use  $A$  to denote the adjacency matrix (binary or weighted) of a network  $G$  with  $N$  nodes and  $M$  edges.  $A(i, :)$  and  $A(:, i)$  stand for its  $i$ th row and column, respectively.  $A(i, j)$  is the weight of the edge between nodes  $i$  and  $j$ .  $A$  is symmetric,  $A^T$  denotes the transpose of  $A$ . Functions are marked by curlicue, e.g.  $\mathcal{F}(\cdot)$ .

**Definition 1.** High-order proximity. Given the adjacency matrix  $A$  of an undirected network, a high-order proximity is defined as a polynomial function  $\mathcal{F}(\cdot)$  of  $A$ :

$$S = \mathcal{F}(A) = w_1 A + w_2 A^2 + \dots + w_q A^q, \quad (1)$$

where  $q$  is the order and  $w_1, \dots, w_q$  are the weights. We refer to a proximity of order  $q$  as the weighted combination of all the orders from the 1st to the  $q$ th, rather than the  $q$ th order alone. We allow  $q = +\infty$  if the

summation converges. We will assume that  $w_i \geq 0$  for  $\forall 1 \leq i \leq q$ . To preserve the high-order proximity in a low-dimensional vector space, the widely adopted method is matrix factorization, which minimizes the following objective function:

$$\min_{U^*, V^*} \|S - U^* V^{*T}\|_F^2, \quad (2)$$

where  $U^*, V^* \in \mathbb{R}^{N \times d}$  are content/context embedding vectors and  $d$  is the dimensionality of the space. Without loss of generality, we use  $U^*$  as the content embedding vectors. From Eckart–Young theorem, the global optimal solution to Equation (2) can be obtained by truncated SVD (Eckart and Young, 1936). Specifically, denote  $[U, \Sigma, V]$  as the top- $d$  SVD results of  $S$ , where  $U, V \in \mathbb{R}^{N \times d}$  and each column corresponds to one left/right singular vector, and  $\Sigma \in \mathbb{R}^{d \times d}$  is a diagonal matrix of singular values in descending order. The embeddings can be obtained by multiplying  $\Sigma$  into  $U, V$ :

$$U^* = U\sqrt{\Sigma}, \quad V^* = V\sqrt{\Sigma}. \quad (3)$$

However, directly calculating  $S$  and SVD will be both time and space consuming. Besides, since different networks and targets applications usually require the proximities of different orders, how to shift across different orders is also challenging.

Denote the top- $d$  eigen-decomposition of  $S$  as  $[\Lambda, X]$ , where  $\Lambda \in \mathbb{R}^{d \times d}$  is a diagonal matrix of eigenvalues in descending order of the absolute value,  $X \in \mathbb{R}^{N \times d}$  and each column corresponds to an eigenvector. We can refer  $[\Lambda(i, i), X(:, i)]$ ,  $1 \leq i \leq d$  as an eigen-pair. To solve the SVD problem, we can transform it into an eigen-decomposition problem (Strang, 2006).

**THEOREM 1.** For any symmetric matrix  $S$ ,  $\forall 1 \leq i \leq d$ , we have:

$$\begin{cases} U(:, i) = X(:, i) \\ \Sigma(i, i) = \text{abs}(\Lambda(i, i)) \\ V(:, i) = X(:, i) \text{sign}(\Lambda(i, i)) \end{cases}, \quad (4)$$

where  $\text{abs}(x) = x$  stands for the absolute value function and  $\text{sign}(\cdot)$  is the sign function, i.e.  $\text{sign}(x) = 1$  if  $x > 0$ ,  $\text{sign}(x) = 0$  if  $x = 0$  and  $\text{sign}(x) = -1$  if  $x < 0$ .

Now, we only need to focus on solving the eigen-decomposition of  $S$ .

As proved in Zhang et al. (2018), to calculate the eigen-decomposition on  $S$ , we can follow the eigen-decomposition Reweighting theorem:

**THEOREM 2.** Eigen-decomposition Reweighting. If  $[\lambda, x]$  is an eigen-pair of  $A$ , then  $[\mathcal{F}(\lambda), x]$  is an eigen-pair of  $S = \mathcal{F}(A)$ .

The theorem shows that, without performing the eigen-decomposition on  $S$ , we can obtain the eigen-decomposition results of  $S$  from the eigen-decomposition results of  $A$  by replacing  $\lambda$  with  $\mathcal{F}(\lambda)$ . In fact, the theorem reveals the intrinsic relationship between proximities of different orders. If we regard each eigenvector as a ‘coordinate’ of the nodes in the network and each eigenvalue as a ‘weight’ of the coordinate, then, preserving proximities of different orders is equivalent to reweighting the dimensions.

After the eigen-decomposition reweighting, the order of the eigenvalues may change, including the top- $d$  eigen-decomposition of  $S$  is not necessarily the reweighting of the top- $d$  eigen-decomposition of  $A$ . To tackle the problem (Zhang et al., 2018) proved that the top- $d$  eigen-decomposition of any  $S$  is guaranteed to be the reweighting of the top- $l$  eigen-decomposition of  $A$ , where  $l = \ell(A, d)$  is a function of the network and  $d$ . Thus, to get the top- $d$  eigen-decomposition of any  $\mathcal{F}(\cdot)$ , we need to calculate the top- $l$  eigen-decomposition of  $A$ . Then we can reweight and reorder dimensions and use the top- $d$  after reweighting to derive the embedding vectors. Since the top- $l$  eigen-decomposition of  $A$  is shared by arbitrary-order proximities, we can shift between proximities of



different orders with a low marginal cost by pre-computing the eigen-decomposition.

## 2.4 Deep forest algorithm

After learning the low-dimensional vector representation of drugs and proteins, we utilize the deep forest (Zhou and Feng, 2017) for prediction, which provides an alternative approach to DNNs to learn hyper-level representations in low computing cost. Inspired by the layer-layer processing of raw features in DNNs, deep forest employs a cascade structure, each level of cascade receives feature information processed by its preceding level and outputs its processing results to the next level (Fig. 1). Each level is an ensemble of decision tree forest, such as an ensemble of ensembles. Diversity is crucial for ensemble construction. In this study, we used: (i) two random forests (RFs), (ii) two completely random tree forests and (iii) two gradient boosting tree forests. Each forest contains 500 trees and there are 3000 trees in total. For instance, each forest will produce an estimate of class distribution, by counting the percentage of different classes of training examples at the leaf node where the concerned instance falls, and then averaging across all trees in the same forest. The estimated class distribution forms a class vector, which is then concatenated with the original feature vector to be input to the next level of the cascade (Fig. 1). Herein, there are two classes in binary classification, with each of the six forests producing a 2D class vector. In total, the next level of the cascade will receive 12 ( $=2 \times 6$ ) augmented features.

To reduce the risk of overfitting, class vector produced by each forest is generated by  $k$ -fold cross-validation ( $k=5$ ). In detail, each forest will be used as training data for  $k-1$  times, resulting in  $k-1$  class vectors, which are then averaged to produce the final class vector as augmented features for the next level of cascade. After expanding to a new level, the performance of the whole cascade will be estimated on a validation set, and the training procedure will terminate if there is no significant performance gain. Subsequently, the number of cascade levels is automatically determined. Deep forest employs a multigrained scanning strategy, a sliding window-based approach, to extract local features by scanning raw input to generate a series of local low-dimensional feature vectors. It then trains a series of forests by using those low-dimensional vectors to obtain class distribution of input vectors. More details are provided in previous study (Zhou and Feng, 2017).

## 3 Results

### 3.1 Baseline methods

- NeoDTI: Neural integration of neighbor information for DTI prediction (Wan *et al.*, 2019) is a nonlinear end-to-end learning model that integrates diverse information from heterogeneous networks and automatically learns topology-preserving representations of drugs and targets for prediction.
- deepDTnet: A network-based, deep learning methodology for drug repurposing, which integrates DNN algorithm for network embedding and a PU-matrix completion algorithm for prediction (Zeng *et al.*, 2020).
- RLSWNN: Regularized Least Squares with Weighted Nearest Neighbors (van Laarhoven and Marchiori, 2013), which uses a weighted nearest neighbor procedure for inferring a profile for a drug by using interaction profiles of drugs in the training data.
- KBMF2K: Kernelized Bayesian matrix Factorization method (Gonen, 2012), which uses a kernelized Bayesian matrix factorization with twin kernels to predict DTIs.
- NetLapRLS: An algorithm utilizing the bipartite local model concept (Xia *et al.*, 2010), performs two sets of predictions, including one from the drug side and one from the target side, and then aggregates these predictions to give the final prediction scores for the potential interaction candidates.

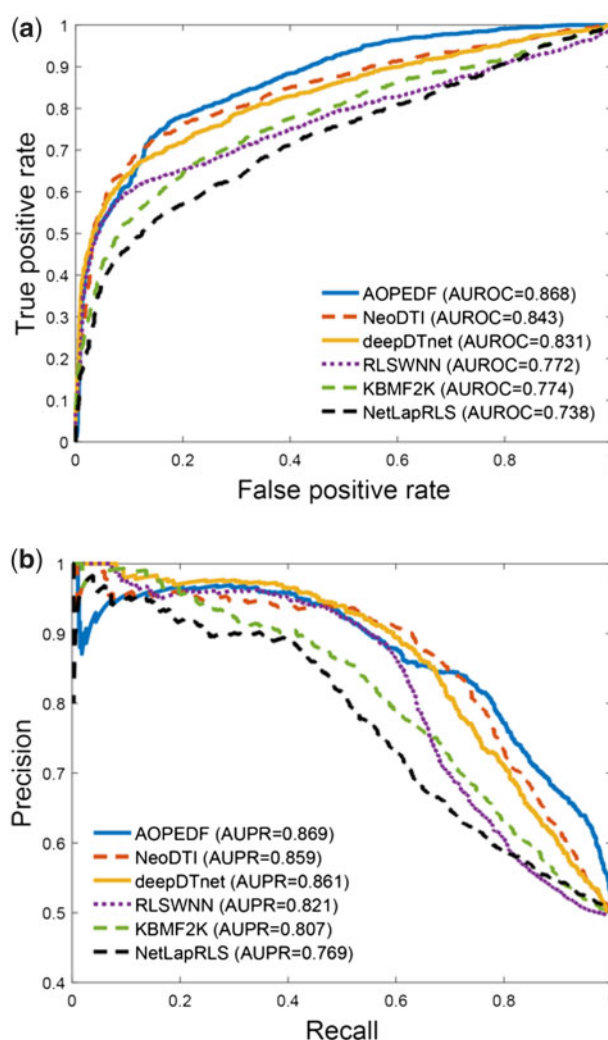


Fig. 2. Evaluation of AOPEDF on the external validation set collected from the DrugCentral database (see Section 2). (a) Receiver operating characteristic (ROC) curves of prediction results obtained by applying AOPEDF and five previously published methods. (b) Precision–recall (PR) curves of prediction results obtained by applying AOPEDF and five previously published methods. AUROC, the area under ROC curve; AUPR, the area under PR curve

- DeepWalk: A deep learning method utilizes the similarities within a heterogeneous tripartite network built from biomedical linked datasets (Zong *et al.*, 2017).

### 3.2 Performance of AOPEDF on the cross-validation

We first evaluated performance of AOPEDF by conducting a 5-fold cross-validation procedure on all positive pairs and a set of matching number of randomly sampled negatives with positive samples (random selection of unknown drug–target pairs by excluding all known DTIs). During each 5-fold cross-validation, we randomly chose a subset of 80% of the known DTI pairs and a matching number of randomly sampled unknown drug–target pairs as the training set, and the remaining 20% known DTI pairs and a matching number of randomly sampled unknown drug–target pairs were held out as the test set. The area under the receiver operating characteristic curve (AUROC) and the area under the precision–recall curve (AUPR) were utilized to evaluate the overall performance of AOPEDF. To reduce the data bias of cross-validation, we performed 10 times of random 5-fold cross-validation and computed the average performance. We found that AOPEDF showed high accuracy (AUROC = 0.985 and AUPR = 0.985) in 5-fold cross-validation, outperforming that of several state-of-the-art methods: NeoDTI (AUROC = 0.971

and AUPR = 0.970), deepDTnet (AUROC = 0.965 and AUPR = 0.969), RLSWNN (AUROC = 0.949 and AUPR = 0.955), KBMF2K (AUROC = 0.936 and AUPR = 0.947) and NetLapRLS (AUROC = 0.923 and AUPR = 0.936) (Supplementary Fig. S1 and Table S4). In addition, AOPEDF outperforms DeepWalk (Zong *et al.*, 2017), a state-of-the-art deep learning approach (Supplementary Fig. S2).

### 3.3 Performance of AOPEDF on the external validation

Cross-validation on retrospective data probably leads to overoptimistic results. For object performance evaluation, we further collected experimentally validated DTIs from DrugCentral and ChEMBL databases, as two external validation sets (Supplementary Table S3), which can be used to evaluate the generalizable ability of models. The DrugCentral validation set contains 1507 DTIs that were not used in the training set, while the ChEMBL validation set contains 3034 DTIs that were not used in the training set as well. Figure 2a and b illustrates the performance comparison from the DrugCentral validation set. AOPEDF achieves a higher performance over other methods in terms of both AUROC and AUPR. Specifically, AOPEDF achieves AUROC value of 0.868, outperforming that of NeoDTI (0.843), deepDTnet (0.831), RLSWNN (0.772), KBMF2K (0.774) and NetLapRLS (0.738). AOPEDF achieves AUPR value of 0.869, outperforming that of NeoDTI (0.859), deepDTnet (0.861), RLSWNN (0.821), KBMF2K (0.807) and NetLapRLS (0.769) as well. Figure 3a and b shows the performance comparison on the ChEMBL validation set. AOPEDF still yields the best prediction performance in comparison with the other methods. AOPEDF achieves an AUROC value of 0.768 in comparison to NeoDTI (0.744), deepDTnet (0.702), RLSWNN (0.692), KBMF2K (0.648) and NetLapRLS (0.593). AOPEDF achieves an AUPR value of 0.764, outperforming that of NeoDTI (0.745), deepDTnet (0.739), RLSWNN (0.722), KBMF2K (0.684) and NetLapRLS (0.642). However, there are partly overlap between two external validation sets (Supplementary Table S3). The generalizable ability of AOPEDF is warranted to be tested further using more independent validation sets in the future.

### 3.4 Performance of AOPEDF by ablation analysis

AOPEDF contains two parts, that is, AROPE for feature extraction and deep forest for classification. To examine the contribution of each component, we compared AOPEDF with several combinations. First, we replaced AROPE with LINE (Tang *et al.*, 2015) for feature extraction. Specifically, we integrated 15 networks using AROPE and LINE respectively, and then used the deep forest for prediction. LINE is another network embedding method, which explicitly preserves the first two order proximities, here denoted as LINE<sub>1st</sub> and LINE<sub>2nd</sub>, respectively. This operation can inspect the contribution of AROPE. As shown in Supplementary Table S5, we found that AROPE outperformed both LINE<sub>1st</sub> and LINE<sub>2nd</sub>. This finding suggested that preserved high-order proximities may provide more effective information for classification. To inspect the contribution of deep forest, we compare deep forest classifier with other traditional classifiers using the same features extracted from AROPE. Specifically, for support vector machine (SVM) (Chang and Lin, 2011), we use a soft margin SVM with linear kernel, which performed better than radial basis function kernel in our experiments. We used a standard RF with 1000 trees, which get the best performance. For DNN (LeCun *et al.*, 2015), we use an MLP having three hidden layers, with 1000, 500 and 200 units, respectively. We use ReLU as activation function and Adam optimizer with learning rate 0.001 to perform gradient descent. The evaluation results of these combinations are reported in Supplementary Table S5. We found that deep forest achieved the best performance. We also evaluated the combination of LINE with traditional classifiers, from which we can further validate the contribution of AROPE and deep forest. In addition, we found that performance of assembling in total 15 networks is much higher than single networks under AOPEDF framework (Supplementary Table S6), indicating power of heterogeneous biological network integration. However, when we left

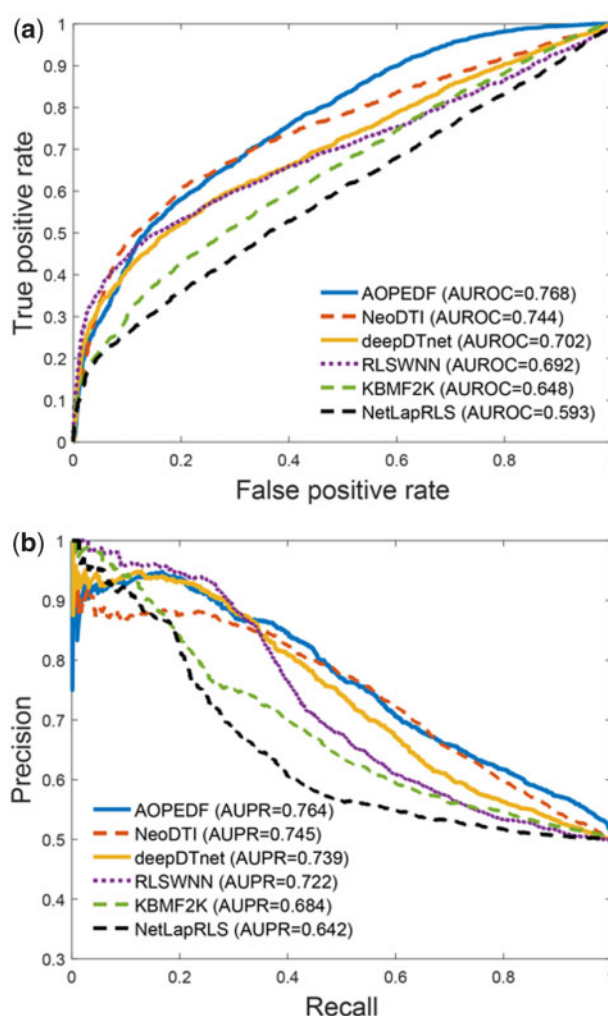


Fig. 3. Evaluation of AOPEDF on the external validation set collected from the ChEMBL database (see Section 2). (a) ROC curves of prediction results obtained by applying AOPEDF and five previously published methods. (b) PR curves of prediction results obtained by applying AOPEDF and five previously published methods. AUROC, the area under ROC curve; AUPR, the area under PR curve

each network out, we only found the marginal improvement of in total 15 networks compared to 14 networks (Supplementary Table S7).

### 3.5 Case study: drug repurposing for substance abuse disorder

Substance abuse disorder, also termed drug addiction, is a serious public health issue and there are no effective treatments available in the clinic (Lo Coco *et al.*, 2019). We next turn to inspect whether AOPEDF could identify molecular targets from marketed drugs in the potential treatment of substance abuse disorder. Here, we centered on 64 G-protein-coupled receptors (GPCRs) which are related to substance abuse disorder (Chen *et al.*, 2019). In total, we computationally identify 648 potential interactions connecting 64 GPCRs and 732 known drugs based on the top 20 predicted candidates by AOPEDF. The network visualization of the top 20 predicted candidates of 64 GPCRs is illustrated in Figure 4. Among the AOPEDF-predicted DTIs, multiple candidates can be supported by previous published literatures. For instance, aripiprazole, an atypical antipsychotic medication, primarily used in the treatment of schizophrenia and bipolar disorder, was predicted by AOPEDF to interact with histamine H3 receptors (HRH3). Such a prediction can be supported by a systematic, unbiased GPCR experimental assay (Lounkine *et al.*, 2012). Besides, we also found that aripiprazole is related to



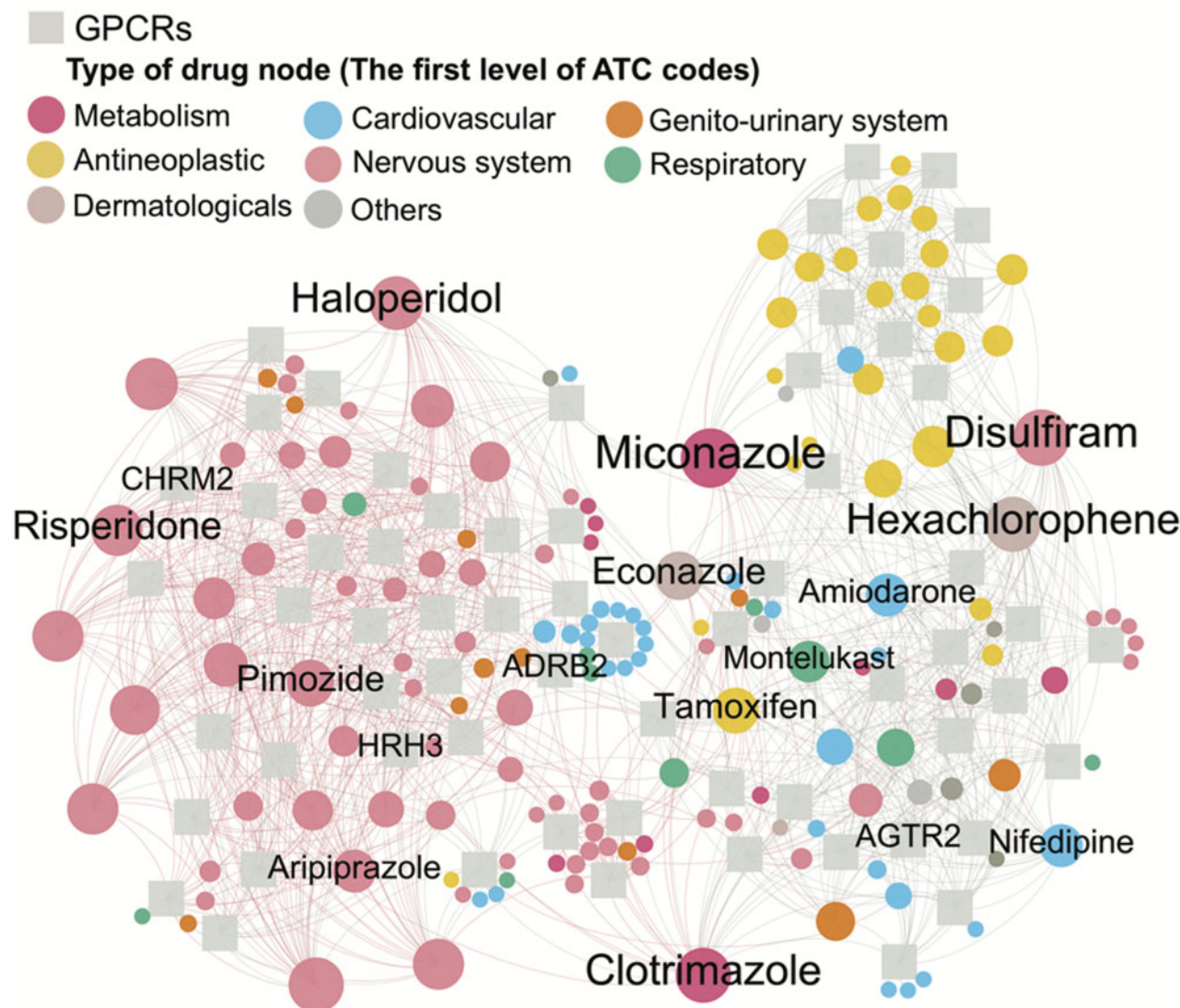


Fig. 4. An AOPEDF-predicted drug–target network connects 64 substance abuse disorder-related GPCRs and 164 drugs. GPCRs are denoted by gray square nodes. Drug nodes (circle) are labeled by the first-level of the Anatomical Therapeutic Chemical Classification System. Node size represents the degree (connectivity). Several GPCRs and predicted drugs were highlighted and discussed in the main text

drug abuse (Brunetti *et al.*, 2012). Risperidone, an atypical anti-psychotic, is approved to treat schizophrenia, bipolar disorder and irritability associated with autism. Here, we computationally identified that risperidone has potential interactions with HRH3 as well predicted by AOPEDF. This prediction is supported by the previous finding that HRH3 was involved in the pharmacodynamics and clinical efficacy of risperidone (Wei *et al.*, 2012). In addition, risperidone was reported to mediate preclinical efficacy of substance abuse (Machielsen and de Haan, 2009). Haloperidol is a typical anti-psychotic medication used in the treatment of schizophrenia, tics in Tourette syndrome, mania in bipolar disorder, nausea and vomiting, delirium, agitation, acute psychosis and hallucinations in alcohol withdrawal. AOPEDF predicts that haloperidol interacts with cholinergic muscarinic 2 receptor, which is also supported by a previous publication (Swathy and Banerjee, 2017). Furthermore, haloperidol was reported to involve in potential treatment of drug abuse as well (Hoffman *et al.*, 1986). In summary, these case studies suggest potential of identifying new molecular targets from marketed drugs in potential treatment of substance abuse disorder. All predictions warrant further preclinical and clinical validations. From a translational perspective, if broadly applied, AOPEDF developed here could help

accelerate therapeutic development for multiple understudied diseases as well.

#### 4 Discussion and conclusion

In this article, we proposed a deep learning-based computational approach for molecular target identification from known drugs, termed AOPEDF. AOPEDF preserves different order proximity information from 15 networks in a constructed drug–target/protein–disease heterogeneous network. Specifically, AOPEDF formulates DTI prediction as a binary classification task and feeds the low-dimensional but informative vector representations of features for both drugs and proteins into a cascade deep forest classifier. The low-dimensional feature vectors learned by AOPEDF capture rich context information as well as the topological structure of individual networks. In comparison to DNNs approaches, the deep forest classifier of AOPEDF performs excellently in classification but has much fewer hyper-parameters and its performance is quite robust to hyper-parameter settings. Neural network methods often achieve state-of-the-art performance with a ‘black-box’, for which the

reasons underlying a prediction cannot be explicitly presented. AOPEDF makes prediction by inferring decision rules from data, which is more effective in generating interpretable predictions from biologically relevant features. We have validated the prediction ability of AOPEDF in terms of 5-fold cross-validation, two external validation sets and a case study. Systematic evaluation demonstrates that AOPEDF achieves state-of-the-art performance for the discovery of DTIs and potential applications of target-centered drug repurposing for substance abuse disorder in the case study. Theoretically, AOPEDF can process various high-dimensional features by utilizing multiple networks with different order features. The deep forest classifier implemented in AOPEDF will utilize the information it needs automatically. In our experiments, for each network we preserve different order proximity, and then choose the best order according to the feature importance and prediction results. Overall, AOPEDF is a scalable framework, which can incorporate more drug and target-related information from various publicly available databases and literatures. Therefore, if broadly applied, we believe that AOPEDF offers a powerful and useful tool to facilitate drug repurposing and therapeutic development in various understudied diseases.

We acknowledged several potential limitations in current study. In this study, we used a low binding affinity value of  $10\ \mu\text{M}$  as a threshold to define a physical DTI. Recent studies suggested that weak-binding drugs play crucial roles in therapeutic development as well (Ohlson, 2008; Wang *et al.*, 2017). Our recent studies have successfully applied this low binding affinity cutoff of  $10\ \mu\text{M}$  for drug repurposing (Cheng *et al.*, 2018, 2019a, b). However, a stronger binding affinity threshold (e.g.  $1\ \mu\text{M}$ ) may be a more suitable cutoff in drug discovery although it will generate a small size of drug–target network (Pahikkala *et al.*, 2015). In addition, random selection of unknown drug–target pairs as negative samples may generate possible false positive rate of AOPEDF models. We have repeated the 10 times of random 5-fold cross-validation on each method and added the mean and standard deviation in the [Supplementary Table S4](#). We found that AOPEDF revealed the smallest standard derivation compared to other approaches, suggesting a minor influence of low-quality negative samples on performance. Building regression models to predict the continuous binding affinity (such as  $K_d$ ,  $K_i$ ,  $\text{IC}_{50}$ ,  $\text{EC}_{50}$ ) will avoid selecting different biological threshold and avoiding lack of publicly available negative drug–target pairs as well. We found that performance of 5-fold cross-validation ([Supplementary Fig. S1](#)) was much higher than performance of two external validation sets ([Figs 2 and 3](#)). One possible reason is that experimental assays of DTIs are different between training set and the external validation sets. However, the overfitting risk of AOPEDF is needed to be tested by more independent validation sets in the future. Ablation analysis reveals a marginal improvement of in total 15 networks compared to 14 networks ([Supplementary Table S7](#)). Thus, potential risk of information redundancy from multiple networks' integration is warranted to be tested further. Other feature extraction approaches, such as convolution neural networks (LeCun *et al.*, 2015), could be used to avoid information redundancy in current AOPEDF framework. Finally, the deep forest classifier has much fewer hyper-parameters compared to DNN algorithms, potentially making the proposed method more robust to parameter settings. As shown in the [Supplementary Table S8](#), AOPEDF reveals high robustness by the hyper-parameter settings. Finally, all experimentally validated drug–target networks, including training set and two external validation sets, and codes used in this study are free available at <https://github.com/ChengF-Lab/AOPEDF>.

## Funding

This work was supported by the National Heart, Lung, and Blood Institute of the National Institutes of Health under Award Number K99HL138272 and R00HL138272 to F.C. This work has been also supported in part with Federal funds from the Frederick National Laboratory for Cancer Research, National Institutes of Health, under contract HHSN261200800001E. This research was supported (in part) by the Intramural Research Program of NIH,

Frederick National Lab, Center for Cancer Research. The content of this publication does not necessarily reflect the views or policies of the Department of Health and Human Services, nor does mention of trade names, commercial products or organizations imply endorsement by the US Government.

*Conflict of Interest:* none declared.

## References

- Apweiler, R. *et al.* (2004) UniProt: the universal protein knowledgebase. *Nucleic Acids Res.*, **32**, D115–119.
- Bleakley, K. and Yamanishi, Y. (2009) Supervised prediction of drug–target interactions using bipartite local models. *Bioinformatics*, **25**, 2397–2403.
- Brunetti, M. *et al.* (2012) Aripiprazole, alcohol and substance abuse: a review. *Eur. Rev. Med. Pharmacol. Sci.*, **16**, 1346–1354.
- Cao, S. *et al.* (2015) GraRep: learning graph representations with global structural information. In: *Proceedings of the 24th ACM International Conference on Information and Knowledge Management*. ACM, Melbourne, Australia, pp. 891–900.
- Chang, C.-C. and Lin, C.-J. (2011) LIBSVM: a library for support vector machines. *ACM Trans. Intell. Syst. Technol.*, **2**, 1–27.
- Chen, M. *et al.* (2019) DAKB-GPCRs: an integrated computational platform for drug abuse related GPCRs. *J. Chem. Inf. Model.*, **59**, 1283–1289.
- Cheng, A.C. *et al.* (2007) Structure-based maximal affinity model predicts small-molecule druggability. *Nat. Biotechnol.*, **25**, 71–75.
- Cheng, F. *et al.* (2012a) Prediction of chemical–protein interactions network with weighted network-based inference method. *PLoS One*, **7**, e41064.
- Cheng, F. *et al.* (2012b) Prediction of drug–target interactions and drug repositioning via network-based inference. *PLoS Comput. Biol.*, **8**, e1002503.
- Cheng, F. *et al.* (2018) Network-based approach to prediction and population-based validation of *in silico* drug repurposing. *Nat. Commun.*, **9**, 2691.
- Cheng, F. *et al.* (2019a) A genome-wide positioning systems network algorithm for *in silico* drug repurposing. *Nat. Commun.*, **10**, 3476.
- Cheng, F. *et al.* (2019b) Network-based prediction of drug combinations. *Nat. Commun.*, **10**, 1197.
- Cui, P. *et al.* (2019) A survey on network embedding. *IEEE Trans. Knowl. Data Eng.*, **31**, 833–852.
- Donald, B.R. (2011) *Algorithms in Structural Molecular Biology*. MIT Press, Cambridge, MA.
- Eckart, C. and Young, G. (1936) The approximation of one matrix by another of lower rank. *Psychometrika*, **1**, 211–218.
- Gaulton, A. *et al.* (2012) ChEMBL: a large-scale bioactivity database for drug discovery. *Nucleic Acids Res.*, **40**, D1100–1107.
- Gonen, M. (2012) Predicting drug–target interactions from chemical and genomic kernels using Bayesian matrix factorization. *Bioinformatics*, **28**, 2304–2310.
- Haggarty, S.J. *et al.* (2003) Multidimensional chemical genetic analysis of diversity-oriented synthesis-derived deacetylase inhibitors using cell-based assays. *Chem. Biol.*, **10**, 383–396.
- He, Z. *et al.* (2010) Predicting drug–target interaction networks based on functional groups and biological features. *PLoS One*, **5**, e9603.
- Hernandez-Boussard, T. *et al.* (2007) The pharmacogenetics and pharmacogenomics knowledge base: accentuating the knowledge. *Nucleic Acids Res.*, **36**, D913–D918.
- Hoffman, A.S. *et al.* (1986) Catatonic reaction to accidental haloperidol overdose: an unrecognized drug abuse risk. *J. Nerv. Ment. Dis.*, **174**, 428–430.
- Keiser, M.J. *et al.* (2007) Relating protein pharmacology by ligand chemistry. *Nat. Biotechnol.*, **25**, 197–206.
- Kuruvilla, F.G. *et al.* (2002) Dissecting glucose signalling with diversity-oriented synthesis and small-molecule microarrays. *Nature*, **416**, 653–657.
- Law, V. *et al.* (2014) DrugBank 4.0: shedding new light on drug metabolism. *Nucleic Acids Res.*, **42**, D1091–D1097.
- LeCun, Y. *et al.* (2015) Deep learning. *Nature*, **521**, 436–444.
- Liu, T. *et al.* (2007) BindingDB: a web-accessible database of experimentally determined protein–ligand binding affinities. *Nucleic Acids Res.*, **35**, D198–201.
- Lo Coco, G. *et al.* (2019) Group treatment for substance use disorder in adults: a systematic review and meta-analysis of randomized-controlled trials. *J. Subst. Abuse Treat.*, **99**, 104–116.
- Lounkine, E. *et al.* (2012) Large-scale prediction and testing of drug activity on side-effect targets. *Nature*, **486**, 361–367.

- Machielsen, M.W. and de Haan, L. (2009) Differences in efficacy on substance abuse between risperidone and clozapine supports the importance of differential modulation of dopaminergic neurotransmission. *Psychopharmacol. Bull.*, **42**, 40–52.
- Mei, J.P. et al. (2013) Drug–target interaction prediction by learning from local information and neighbors. *Bioinformatics*, **29**, 238–245.
- Mendez, D. et al. (2019) ChEMBL: towards direct deposition of bioassay data. *Nucleic Acids Res.*, **47**, D930–D940.
- Morris, G.M. et al. (2009) AutoDock4 and AutoDockTools4: automated docking with selective receptor flexibility. *J. Comput. Chem.*, **30**, 2785–2791.
- Ohlson, S. (2008) Designing transient binding drugs: a new concept for drug discovery. *Drug Discov. Today*, **13**, 433–439.
- Pahikkala, T. et al. (2015) Toward more realistic drug–target interaction predictions. *Brief. Bioinform.*, **16**, 325–337.
- Pawson, A.J. et al. (2014) The IUPHAR/BPS Guide to PHARMACOLOGY: an expert-driven knowledgebase of drug targets and their ligands. *Nucleic Acids Res.*, **42**, D1098–D1106.
- Perlman, L. et al. (2011) Combining drug and gene similarity measures for drug–target elucidation. *J. Comput. Biol.*, **18**, 133–145.
- Perozzi, B. et al. (2014) DeepWalk: online learning of social representations. In: *Proceedings of the 20th ACM SIGKDD International Conference on Knowledge Discovery and Data Mining*. ACM, New York, NY, USA, pp. 701–710.
- Rarey, M. et al. (1996) A fast flexible docking method using an incremental construction algorithm. *J. Mol. Biol.*, **261**, 470–489.
- Strang, G. (2006) *Linear Algebra and Its Applications*, 4th edn. India Edition. ISBN-10: 9788131501726.
- Swathy, B. and Banerjee, M. (2017) Haloperidol induces pharmacoeigenetic response by modulating miRNA expression, global DNA methylation and expression profiles of methylation maintenance genes and genes involved in neurotransmission in neuronal cells. *PLoS One*, **12**, e0184209.
- Tang, J. et al. (2015) LINE: large-scale information network embedding. In: *Proceedings of the 24th International Conference on World Wide Web*. International World Wide Web Conferences Steering Committee, Florence, Italy, pp. 1067–1077.
- Ursu, O. et al. (2019) DrugCentral 2018: an update. *Nucleic Acids Res.*, **47**, D963–D970.
- van Laarhoven, T. and Marchiori, E. (2013) Predicting drug–target interactions for new drug compounds using a weighted nearest neighbor profile. *PLoS One*, **8**, e66952.
- Wan, F. et al. (2019) NeoDTI: neural integration of neighbor information from a heterogeneous network for discovering new drug–target interactions. *Bioinformatics*, **35**, 104–111.
- Wang, J. et al. (2017) Weak-binding molecules are not drugs? Toward a systematic strategy for finding effective weak-binding drugs. *Brief. Bioinform.*, **18**, 321–332.
- Wang, W. et al. (2014) Drug repositioning by integrating target information through a heterogeneous network model. *Bioinformatics*, **30**, 2923–2930.
- Wei, Z. et al. (2012) A pharmacogenetic study of risperidone on histamine H3 receptor gene (HRH3) in Chinese Han schizophrenia patients. *J. Psychopharmacol.*, **26**, 813–818.
- Wishart, D.S. et al. (2018) DrugBank 5.0: a major update to the DrugBank database for 2018. *Nucleic Acids Res.*, **46**, D1074–D1082.
- Xia, Z. et al. (2010) Semi-supervised drug–protein interaction prediction from heterogeneous biological spaces. *BMC Syst. Biol.*, **4**(Suppl. 2), S6.
- Yang, H. et al. (2016) Therapeutic target database update 2016: enriched resource for bench to clinical drug target and targeted pathway information. *Nucleic Acids Res.*, **44**, D1069–D1074.
- Zeng, X. et al. (2020) Target identification among known drugs by deep learning from heterogeneous networks. *Chem. Sci. In press*. DOI: 10.1039/C9SC04336E.
- Zhang, Z. et al. (2018) Arbitrary-order proximity preserved network embedding. In: *Proceedings of the 24th ACM SIGKDD International Conference on Knowledge Discovery and Data Mining*. ACM, London, UK, pp. 2778–2786.
- Zheng, X. et al. (2013) Collaborative matrix factorization with multiple similarities for predicting drug–target interactions. In: *Proceedings of the 19th ACM SIGKDD International Conference on Knowledge Discovery and Data Mining*. ACM, Chicago, IL, USA, pp. 1025–1033.
- Zhou, Z.-H. and Feng, J. (2017) Deep forest: towards an alternative to deep neural networks. In: *Proceedings of the Twenty-sixth International Joint Conference on Artificial Intelligence*. South Wharf, Australia, pp. 3553–3559.
- Zong, N. et al. (2017) Deep mining heterogeneous networks of biomedical linked data to predict novel drug–target associations. *Bioinformatics*, **33**, 2337–2344.